

## Neutron halo of ${}^6\text{He}$ in a microscopic model

Attila Csótó\*

*Institute of Nuclear Research of the Hungarian Academy of Sciences, P.O. Box 51, Debrecen, H-4001, Hungary*  
(Received 8 March 1993)

The two-neutron separation energy of  ${}^6\text{He}$  has been reproduced for the first time in a realistic parameter-free microscopic multicluster model comprising the  $\alpha + n + n$  and  $t + t$  clusterizations, with  $\alpha$  cluster breathing excitations included. The contribution of the  $t + t$  channel is substantial. A very thick (0.85 fm) neutron halo has been found in full agreement with the results of the latest phenomenological analysis.

PACS number(s): 21.10.-k, 21.30.+y, 21.60.Gx, 27.20.+n

### I. INTRODUCTION

Recently nuclei far from stability attract much interest in nuclear physics. Prominent representatives of these nuclei are, e.g.,  ${}^6\text{He}$ ,  ${}^8\text{He}$ ,  ${}^8\text{Li}$ ,  ${}^8\text{B}$ ,  ${}^{11}\text{Li}$ . There are several calculations for their description in macroscopic [1–4], semimicroscopic [5], and microscopic [6] models. In this paper we use our dynamical microscopic multiconfiguration multicluster model, developed and applied recently to the ground state of  ${}^6\text{Li}$  [7], to study the neutron halo structure of the ground state of  ${}^6\text{He}$ . All realistic macroscopic three-body models underbind  ${}^6\text{He}$  by about 0.6–0.3 MeV. The situation is similar to  ${}^{11}\text{Li}$ , which is predicted to be unbound by the most realistic parameter-free variational calculation [2]. Our first aim is to check the validity of these models by comparing them with our microscopic model, and to understand the physics of this underbinding. Secondly, we calculate the thickness of the neutron halo of  ${}^6\text{He}$ . For this quantity there are two contradicting experimental predictions, both of them are based on Glauber-type analyses of certain reaction cross-section data. A simpler analysis gives  $\sim 0.4$  fm [8], while the other one, which comes from more realistic model assumptions, results in  $\sim 0.9$  fm [9]. The latter result is well reproduced in a relativistic mean field model [9].

As we shall see, our model strongly supports the second prediction, too.

As the  $\alpha$  particle is an inert cluster, it is natural to assume that an  $\alpha + n + n$  model is a most adequate one for the description of  ${}^6\text{He}$ . This nucleus is said to be borromean [10], which means that after the removal of any of the three clusters, the remaining nucleus decays into two fragments. This indicates that  ${}^6\text{He}$  has a genuine three-body nature and explains why the macroscopic three-body models are so successful in describing its ground-state structure and reactions [10]. Although several physical quantities have been calculated, and a good overall agreement with experiment has been reached in these models, it is necessary to investigate the validity of their foundation starting from microscopic grounds, because nucleon exchange and cluster rearrangement effects are expected to be important in this mass range.

### II. MODEL

The microscopic dynamical multiconfiguration three-cluster model starts from the following trial function for the six-body problem:

$$\begin{aligned} \Psi &= \sum_{S,l_1,l_2,L} \Psi_{S,(l_1l_2)L}^{\alpha(nn)} + \sum_{S,l_1,l_2,L} \Psi_{S,(l_1l_2)L}^{n(\alpha n)} \\ &= \sum_{S,l_1,l_2,L} \sum_i^{N_c} \mathcal{A} \left\{ \left[ [\Phi_i^\alpha (\Phi^n \Phi^n)]_S [\chi_{il_1}^{nn}(\rho_{nn}) \chi_{il_2}^{\alpha(nn)}(\rho_{\alpha(nn)})]_L \right]_{JM} \right\} \\ &\quad + \sum_{S,l_1,l_2,L} \sum_i^{N_c} \mathcal{A} \left\{ \left[ [\Phi^n (\Phi_i^\alpha \Phi^n)]_S [\chi_{il_1}^{\alpha n}(\rho_{\alpha n}) \chi_{il_2}^{n(\alpha n)}(\rho_{n(\alpha n)})]_L \right]_{JM} \right\} \end{aligned} \quad (1)$$

Here  $\mathcal{A}$  is the intercluster antisymmetrizer, the  $\rho$  vectors are the different intercluster Jacobi coordinates, and  $[ ]$  denotes angular momentum coupling. While  $\Phi^n$  is

a neutron spin-isospin eigenstate,  $\Phi_i^\alpha$  denote the ground state and some excited states of the antisymmetrized  $\alpha$  particle, and has the form

$$\Phi_i^\alpha = \sum_{j=1}^{N_c} A_{ij} \phi_{\beta_j}^\alpha, \quad i = 0, 1, \dots, (N_c - 1), \quad (2)$$

\*Contact e-mail address: H988CSO@ELLA.HU

where  $\phi_{\beta_j}^\alpha$  is a translation invariant shell-model state of the  $\alpha$  particle with size parameter  $\beta_j$  and the  $A_{ij}$  parameters are to be determined by minimizing the energy of the  $\alpha$  particle [11]. In the literature the models using such internal states for the description of the free clusters are called distortion models [11] or breathing cluster models [12]. This allows us to take into account the distortion of the  $\alpha$  particle caused by the two outer neutrons. The contribution of this distortion effect to the binding energy of  ${}^6\text{He}$  yields information about the role of the  $\alpha$ -breaking rearrangement channels. Putting (1) into the six-nucleon Schrödinger equation we arrive at an equation for the intercluster relative motion functions  $\chi$ . These functions are expanded in terms of the so-called tempered Gaussian functions [13] with different ranges. For example, in the case of  $\chi_{i,lm}^{\alpha n}(\rho_{\alpha n})$

$$\chi_{i,lm}^{\alpha n}(\rho_{\alpha n}) = \sum_{k=1}^{N_{\alpha n}} c_{ik} \Gamma_{lk}^{\alpha n}(\rho_{\alpha n}), \quad (3)$$

where

$$\Gamma_{lk}^{\alpha n}(\rho_{\alpha n}) = \left( \frac{2^{l+1} (2\nu_k)^{l+3/2}}{\sqrt{\pi} (2l+1)!!} \right)^{1/2} \rho_{\alpha n}^l e^{-\nu_k \rho_{\alpha n}^2} Y_{lm}(\hat{\rho}_{\alpha n}) \quad (4)$$

and the coefficients  $c_{ik}$  are to be determined from a variational principle with Eq. (1) as a trial function. The use of the tempered Gaussian functions makes it possible to calculate all necessary matrix elements analytically. The present microscopic model is the same in many respects as was used in [7] for the ground state of  ${}^6\text{Li}$ .

Thus we describe  ${}^6\text{He}$  as a superposition of the  $\alpha(nn)$  and  $n(\alpha n)$  partitions with a distortable  $\alpha$  particle being in a spin-isospin zero state. The  $J^\pi=0^+$  ground state of  ${}^6\text{He}$  allows only the  $(L, S) = (0, 0)$  and  $(1, 1)$  states to contribute. In the  $[S, (l_1 l_2) L] J$  coupling scheme we take into account all important components that have any significance in the binding energy. It is found that, if restricted to the  $\alpha + n + n$  space, from the point of view of the energy it is enough to include the following terms in the trial function:

$$\Psi = \Psi_{0,(00)0}^{\alpha(nn)} + \Psi_{1,(11)1}^{\alpha(nn)} + \Psi_{0,(00)0}^{n(\alpha n)} + \Psi_{0,(11)0}^{n(\alpha n)} + \Psi_{1,(11)1}^{n(\alpha n)}. \quad (5)$$

Obviously, the role of the presence of the  $n(\alpha n)$  type clusterizations [second term on the right-hand side of (1)] is that in the  $\alpha(nn)$  configuration we can drop the higher angular momentum components [e.g.,  $0,(22)0$ ;  $0,(44)0$ ;...] which components, however, are non-negligible in certain macroscopic three-body models [1, 3], which only include the  $\alpha(nn)$  type configurations. This finding has been confirmed by test calculations. In this paper we use the same  $\nu$  parameters in Eq. (4) as were used in [7] for the  $N + N$  and  $\alpha + N$  relative motions, respectively. Several test calculations show, however, that, if the model space is “complete enough,” as in our case, the results are independent of the choice of the basis pa-

rameters, whenever the basis is well balanced and spatially extensive enough.

### III. INTERACTION

In microscopic calculations the choice of the effective  $N$ - $N$  interaction is a crucial point. If one wants a model to have anything to do with the real physical problem in question, one must be sure that the  $N$ - $N$  interaction is appropriate for all subsystems which appear in the model. We must emphasize that from this point of view the macroscopic approaches are in a more favorable position. While in microscopic models the interaction is strongly constrained by the state spaces assigned to the cluster internal motions, which fact manifests itself in that the bulk properties of the free clusters must be more or less reproduced, in macroscopic approaches the binding energies and the rms radii of the free clusters not even appear explicitly. Since the  $\{\alpha(nn); 0, (00)0\}$  configuration is expected to have a significant role in  ${}^6\text{He}$ , one of the important subsystems we have to pay attention to is the  ${}^{2S+1}L_J = {}^1S_0$  singlet  $N + N$  state. This is an antibound state with negative energy but at the same time with negative imaginary wave number [14]. It means that the specification of this state by its energy is not sufficient. One can distinguish between the bound and antibound states only by an analysis of the scattering phase shift or by the determination of the pole position of the  $S$  matrix of the  $N + N$  scattering or by looking into the effective-range parameters. Most of the published effective  $N$ - $N$  interactions in the cluster model literature do not take special care of this state. Those that contain only space exchanges (i.e., only Majorana parameter) in addition to a Wigner force are definitely inappropriate because if they bind the triplet deuteron, they bind the  ${}^1S_0$  singlet dinucleon states, too. That is, they produce a bound singlet dineutron which contradicts the borromean nature of  ${}^6\text{He}$ . A very popular potential family of such kind are the Volkov forces [15].

There are few cases where definite attention has been paid to this  ${}^1S_0$  state during the construction of the interaction. In [16] the aim was to find an effective  $N$ - $N$  force which gives good results for the two-nucleon systems comparable with the results of realistic forces (e.g., [17]). But at the same time the quality of the description of other nuclei (e.g., the  $\alpha$  particle) with this force has not been investigated. We have done a pilot calculation for the  $\alpha$  particle described by a single  $0s$  shell model state which gives correct rms radius for  $\alpha$  and found it unbound by about 20 MeV. The inclusion of a few  $\alpha$  breathing modes makes the situation better but the  $\alpha$  particle still remains unbound. The reason of this failure is obviously the fact that this force would allow the  $D$  state to play significant role in the  $\alpha$  cluster, but our model can handle only  $0s$ -state clusters.

Another interaction is proposed by Tang *et al.* [18]. This reproduces the experimental  $s$ -wave  $p + p$  effective-range parameters, gives realistic results for the bulk properties of all  $0s$ -shell nuclei, and, supplemented by a spin-orbit force [19], reproduces the  $p$ -wave  $\alpha + N$  scattering

phase shifts up to 15 MeV very well. The form of this interaction is

$$V_{ij}(\mathbf{r}) = \left[ V_1 + \frac{1}{2}(1 + P_{ij}^\sigma)V_2 + \frac{1}{2}(1 - P_{ij}^\sigma)V_3 \right] \\ \times \left[ \frac{1}{2}u + \frac{1}{2}(2 - u)P_{ij}^r \right] \\ + \frac{1 - \tau_{iz}}{2} \frac{1 - \tau_{jz}}{2} \frac{e^2}{r_{ij}} + V_4 \hbar^{-1} \mathbf{l} \cdot (\boldsymbol{\sigma}_i + \boldsymbol{\sigma}_j), \quad (6)$$

where  $P^r$  and  $P^\sigma$  are the space- and spin-exchange operators, respectively,  $u$  is the exchange mixture parameter,  $\mathbf{r} = \mathbf{r}_2 - \mathbf{r}_1$ ,  $\tau_{iz}$  are the  $z$  components of the isospin vector,  $\boldsymbol{\sigma}_i$  are the Pauli vectors of the nucleonic spin, and

$$\mathbf{l} = -\frac{1}{2}i\hbar\mathbf{r} \times (\nabla_2 - \nabla_1), \quad (7)$$

is the orbital momentum of the relative motion of the two nucleons. The potentials have the following Gaussian form factors:

$$V_k = V_{0k} \exp(-r_{ij}^2/a_k^2), \quad k = 1, \dots, 4. \quad (8)$$

There are two shortcomings of the Tang force that we should mention. One of them comes from the fact that the description of the two-nucleon states is good only in an effective manner, i.e., the phase shifts are not perfect and in the triplet  $p + n$  case the experimental deuteron energy is reproduced by assuming a pure  ${}^3S_1$  state. The allowance of the coupling between the  ${}^3S_1$  and  ${}^3D_1$  states by the inclusion of a tensor force ruins the picture because it considerably lowers the binding energy of the deuteron. The second problem is that, as a result of the lack of tensor force, the anomalous low energy order, 1,2,0, of the  ${}^3P_J$  ( $J = 0, 1, 2$ ) phase shifts [20] cannot be reproduced (a local central plus spin-orbit  $N-N$  interaction produces 0,1,2 or 2,1,0 order of phase shifts). As far as a  $J^\pi = 0^+$  state is concerned in the six-nucleon system, the first shortcoming does not cause any problem because in this case a triplet  $S$  state between the two outer nucleons cannot be present. However, it can give rise to difficulties, e.g., in the description of the  $1^+$  ground state of  ${}^6\text{Li}$ . Our test calculations show that this really happens. In a model, which contains all possible angular momentum configurations of any significance, this force overbinds the ground state of  ${}^6\text{Li}$  by about 1.2 MeV. To check the effect of the second shortcoming, we supplemented the Tang force by a tensor term due to Heiss and Hackenbroich [21]; this combination gave good results for the five-nucleon systems [22]. We have determined its exchange mixture parameters so as to reproduce the anomalous  ${}^3P_J$   $N + N$  phase shift splitting qualitatively. Since our tensor force is based only on this not very firm ground, we do not use it in  ${}^6\text{He}$  except for test purposes.

Our force parameters are as follows:

$$\begin{aligned} V_{01} &= 200.0 \text{ MeV}, & a_1 &= 0.82006 \text{ fm}, \\ V_{02} &= -178.0 \text{ MeV}, & a_2 &= 1.25098 \text{ fm}, \\ V_{03} &= -91.85 \text{ MeV}, & a_3 &= 1.46647 \text{ fm}, \\ V_{04} &= -591.1 \text{ MeV}, & a_4 &= 0.57735 \text{ fm}. \end{aligned}$$

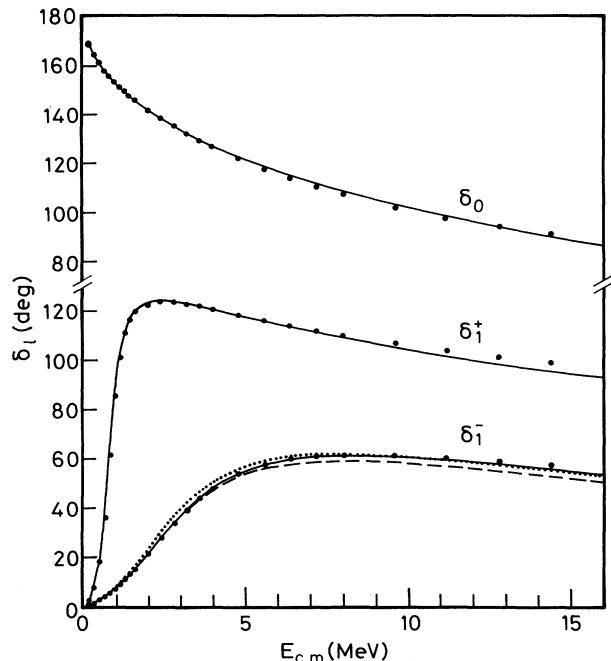


FIG. 1. Phase shifts for  $\alpha + n$  scattering in  $l = 0$  and 1 states (dashed line: in the  $\{\alpha + n + n; t + t\}$  model with  $u = 0.92$ ,  $V_4 = -691.1$  MeV; dotted line: the same model but with  $u = 0.94$ ,  $V_4 = -641.1$  MeV). Experimental data are taken from [23].

We have chosen  $N_C$  in (2) to be 3, which yields the following size parameters:  $\beta_1 = 0.355 \text{ fm}^{-2}$ ,  $\beta_2 = 0.795 \text{ fm}^{-2}$ ,  $\beta_3 = 2.66 \text{ fm}^{-2}$ . The energy and the point matter rms radius of the  $\alpha$  particle are  $-25.60$  MeV and  $1.407$  fm, respectively, to be compared to the experimental values  $-28.296$  MeV and  $1.48$  fm. The exchange mixture parameter  $u$  is set to be  $0.98$  to fit the  $\alpha + N$  phase shifts as are seen in Fig. 1 (further on we show the  $\alpha + n$  and  $p + p$  scattering phase shifts). Owing to the antisymmetrization our model does not produce a bound  $s$  state in the  $\alpha + N$  scattering. Although the theoretical effective-range parameters of the  ${}^1S_0$   $N + N$  state are close to the experiment, the phase shift is not perfect, but the antibound character is very well reproduced (Fig. 2). It is easy to see that in the  $\alpha(nn)$  configuration only the  ${}^3P_1$  triplet-odd  $N + N$  state can be present in the  $J^\pi = 0^+$  state of the six-nucleon system. In this partial wave the agreement with experiment is also fairly good, although the inclusion of the tensor force renders the theoretical results closer to the experiment. It will be shown that higher partial waves in both the  $N + N$  and  $\alpha + N$  relative motions can safely be neglected. We emphasize that all parameters are fixed to independent data, that is, as far as  ${}^6\text{He}$  is concerned, our model is parameter free.

#### IV. RESULTS AND DISCUSSION

The above interaction sets the two-neutron separation energy of the  ${}^6\text{He}$  g.s. at  $0.740$  MeV, which is to be compared to the experimental value  $0.975$  MeV [24]. The

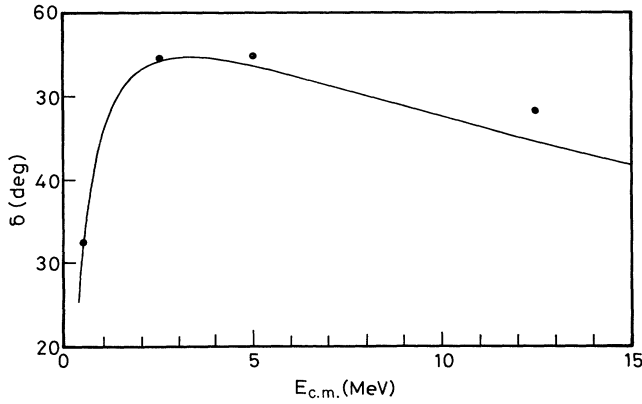


FIG. 2.  $^1S_0$  phase shift of the  $p + p$  scattering. Experimental data are taken from [20].

weights of the  $L = 0, S = 0$  and  $L = 1, S = 1$  components are in Table I, along with the results of [1] and [3]. To quantify the roles of the different nonorthogonal channels we have computed the amounts of clustering  $S_\mu$  of the different clusterizations  $\mu$ . This quantity is the weight of the component of the wave function  $\Psi$  that lies in the segment of the state space associated with clusterization  $\mu$  [25]:

$$S_\mu = \langle \Psi | P_\mu | \Psi \rangle, \quad (9)$$

where  $P_\mu$  projects onto the subspace  $\mu$ . Here we used the method of [7] to calculate  $S_\mu$ . The resulting values are in Table II, while the contribution of the different channels to the energy of  $^6\text{He}$  is in Table III. It is interesting to see that the amount of clustering of the  $\{n(\alpha_0n); 0, (00)0\}$  component is larger than that of  $\{\alpha_0(nn); 0, (00)0\}$  in spite of the fact that the latter contributes much more to the binding energy than the former. This supports the results that in the pure  $\alpha(nn)$  type macroscopic models there are non-negligible components with higher angular momenta [e.g.,  $\{\alpha(nn); 0, (22)0\}$ ]. In our model these components are well represented by the  $n(\alpha n)$  type components. To check this we complemented our model space (5) by  $\Psi_{0,(22)0}^{\alpha(nn)}$  and  $\Psi_{0,(22)0}^{n(\alpha n)}$ . The energy gain is really small, being 0.0025 MeV, and the amounts of these clusterizations are 0.035 for  $\{\alpha_0(nn); 0, (22)0\}$  and 0.015 for  $\{n(\alpha_0n); 0, (22)0\}$ .

For further test purposes we have done calculations for the two other members of the  $J^\pi = 0^+, T = 0$  isospin triplet in  $A = 6$ , namely, on  $^6\text{Li}$  and  $^6\text{Be}$ . Since the g.s. of  $^6\text{Be}$  is unbound, our present method for  $^6\text{Be}$  is a pseudobound-state approximation [26]. In  $^6\text{Be}$  the same components are taken into account as in Eq. (5), while in  $^6\text{Li}$  all  $\alpha(pn)$ ,  $p(\alpha n)$ , and  $n(\alpha p)$  clusterizations are present and in  $\alpha(pn)$  we include the  $0, (11)0$  component as well. The presence of this  $0, (11)0$  component requires the  $^1P_1 N + N$  subsystem to be correct. We checked that our phase shift is close to experiment in this partial wave, too. Table I shows that the deviations from experiment are much larger in [3] than in our case, but our results agree well with the results of [1]. (In [1] no parameter-free results were published for  $^6\text{Li}$  and  $^6\text{Be}$ , but the estimation of the Coulomb energies gave results similar to ours for these nuclei, too.) The situation is similar in respect of the weights, our results being closer to the results of [1]. In contrast with [1], however, in our case the weights of the  $(L, S) = (1, 1)$  component are decreasing from  $^6\text{He}$  to  $^6\text{Be}$ . The origin of this contradicting behavior in microscopic and macroscopic models is not known. The agreement between our results and the results of the best macroscopic model [1] both with respect to the separation energies and the weights of the various  $(L, S)$  components is remarkably good. Since this macroscopic model is also parameter free and the description of the subsystems has similar quality (in [1] the description of the  $N + N$  states is almost perfect but the  $\alpha + N$  phase shifts are worse than ours), this agreement strongly supports the validity of Ref. [1] macroscopic three-body approaches in describing  $^6\text{He}$ .

Having found our model appropriate for  $^6\text{He}$  from the point of view of both energetic and fragmentation properties, the next step is to calculate the thickness of its neutron halo. We have calculated the point nucleon root mean square matter, neutron, and proton radii of  $^6\text{He}$ . The results are presented in Table IV. Although our  $\alpha$  particle is a bit smaller than it should be, which implies that the resulting radii of  $^6\text{He}$  may be smaller by the same amount, the thickness of the neutron halo is not affected by this discrepancy. In our present theoretical model the neutron halo is considerably thicker than the one which was extracted from certain reaction cross-section measurements [8], but is in a very good agreement with the

TABLE I. Energies (relative to the  $\alpha$  energy) and weights of the  $(L, S)$  components of the  $J^\pi = 0^+, T = 1$  isospin triplet in  $A = 6$ .

Model	$^6\text{He} (0^+, T = 1)$			$^6\text{Li} (0^+, T = 1)$			$^6\text{Be} (0^+, T = 1)$		
	$E$ (MeV)	(0,0)	(1,1)	$E$ (MeV)	(0,0)	(1,1)	$E$ (MeV)	(0,0)	(1,1)
Kukulin-86 [3]	-0.138	95.70	4.30	0.742	96.30	3.70	2.083		
Kukulin-92 [3]	-0.025	91.74	8.26	0.844	92.75	7.25	2.102	94.89	5.11
Danilin [1]	-0.731	85.76	14.71	a	84.75	15.26	a	82.33	18.40
$\{\alpha + N_1 + N_2\}^b$	-0.740	86.24	13.76	0.165	87.07	12.93	1.516	87.55	12.46
$\{\alpha + N_1 + N_2; T_1 + T_2\}^c$	-0.961	88.15	11.85	-0.025	88.75	11.25	1.357	89.08	10.92
Experiment [24]	-0.975			0.137			1.371		

<sup>a</sup>No parameter-free data are available.

<sup>b</sup>For  $^6\text{He}$ :  $N_1 = N_2 = n$ ; for  $^6\text{Li}$ :  $N_1 = n, N_2 = p$ ; for  $^6\text{Be}$ :  $N_1 = N_2 = p$ .

<sup>c</sup>For  $^6\text{He}$ :  $T_1 = T_2 = t$ ; for  $^6\text{Li}$ :  $T_1 = t, T_2 = ^3\text{He}$ ; for  $^6\text{Be}$ :  $T_1 = T_2 = ^3\text{He}$ .

TABLE II. Cluster decomposition of  ${}^6\text{He}$  (the three numbers in each group are for the three  $\alpha$  states).

Partition	Clusterization		Amount of clustering	
	$S, (l_1 l_2) L$	$\{\alpha + n + n\}$	$\{\alpha + n + n; t + t\}$	
$\alpha(nn)$	0,(00)0	(0.8378,0.4457,0.0004)	(0.8446,0.4651,0.0006)	
$\alpha(nn)$	1,(11)1	(0.1265,0.0004,0.00003)	(0.1086,0.0003,0.00004)	
$n(\alpha n)$	0,(00)0	(0.8443,0.4696,0.0006)	(0.8491,0.4893,0.0008)	
$n(\alpha n)$	0,(11)0	(0.8424,0.0098,0.0002)	(0.8469,0.0153,0.0003)	
$n(\alpha n)$	1,(11)1	(0.1363,0.0005,0.00006)	(0.1173,0.0005,0.00008)	
$tt$	0,0	0.4964	0.5471	

result of the latest phenomenological analysis [9]. The agreement with [5], where a cluster orbital shell model was used for  ${}^6\text{He}$ , is also remarkable. It is known, however, that the radii trivially depend on the separation energy [27], and our separation energy is not correct. That is why we have to seek further after the possible origin of this energy lack.

The same amount of binding energy lack in microscopic and macroscopic models excludes the possibility that the same mechanism causes the lack of  ${}^6\text{He}$  binding energy as causes the lack of binding energy of the  $\alpha$  particle itself, in microscopic models. To see the role of the breathing modes of the  $\alpha$  particle, we repeated the calculations with  $N_c=1$  in (1). In this case the energy optimized  $\beta$  is  $0.606 \text{ fm}^{-2}$ . The  $\alpha + N$  phase shifts remain almost unchanged (in Fig. 1 they are indistinguishable from the phase shifts of the  $N_c = 3$  case) but the two-neutron separation energy becomes  $0.652 \text{ MeV}$ , i.e., the distortion of the  $\alpha$  particle results in a roughly  $0.09\text{-MeV}$  gain in  ${}^6\text{He}$ . The fact that the  $\alpha$  breathing modes hardly affect the  $\alpha + N$  scattering but substantially contribute to the energy of  ${}^6\text{He}$  makes it probable that the  $\alpha$  breathing modes represent not a two-body on-shell excitation effect, but a three-body off-shell excitation-deexcitation mechanism, i.e., the core polarization of the  $\alpha$  particle. A similar effect has been found in the g.s. of  ${}^6\text{Li}$  [7]. Of course, our finding is not a proof of the presence of core polarization, it should be investigated by further calculations. We mention here that the probable role of core polarization in  ${}^{11}\text{Li}$  was emphasized in [2]. The importance of  $\alpha$  breathing modes indicates that the  $\alpha$ -breakup rearrangement channels may have large weights in  ${}^6\text{He}$ .

TABLE III. Change of  ${}^6\text{He}$  energy (relative to the  $\alpha$  energy) in MeV when each one of the clusterization components is omitted.

Omitted component Partition	Model		
	$S, (l_1 l_2) L$	$\{\alpha + n + n\}$	$\{\alpha + n + n; t + t\}$
None		- 0.740	- 0.961
$\alpha(nn)$	0,(00)0	- 0.429	- 0.638
$\alpha(nn)$	1,(11)1	- 0.708	- 0.924
$n(\alpha n)$	0,(00)0	- 0.736	- 0.957
$n(\alpha n)$	0,(11)0	- 0.643	- 0.876
$n(\alpha n)$	1,(11)1	- 0.294	- 0.488
$tt$	0,0		- 0.315

This is in agreement with the finding of [28], where the important role of the  $t+{}^3\text{He}$  rearrangement channel has been pointed out in the g.s. of  ${}^6\text{Li}$ . The most likely of these channels in  ${}^6\text{He}$  is the  $t+t$  clusterization. As we can see in Table II, the weight of this clusterization is large (0.496) even in a model space which does not contain explicitly a  $t+t$  term.

Therefore we have supplemented our model space (5) by a  $t+t$  term

$$\Psi_{0,0}^{tt} = \mathcal{A} \left\{ \left[ [\Phi^t \Phi^t]_0 \chi_0^{tt}(\rho_{tt}) \right]_{00} \right\}. \quad (10)$$

The energy optimized size parameter of the triton is  $\beta_t = 0.451 \text{ fm}^{-2}$ , which gives  $-4.56 \text{ MeV}$  and  $1.48 \text{ fm}$  for the energy and radius of  $t$ , respectively, to be compared to the experimental values  $-8.482 \text{ MeV}$  and  $1.49 \text{ fm}$ . The inclusion of (10) into the trial function puts the two-neutron separation energy of  ${}^6\text{He}$  from  $0.740 \text{ MeV}$  to  $1.416 \text{ MeV}$ , that is,  ${}^6\text{He}$  becomes overbound by about  $0.44 \text{ MeV}$ . This can be explained by recalling that the effective force tailored for a state space that does not include rearrangement channels is more restrictive than the  $\{\alpha + n + n; t + t\}$  state space. To cure this shortcoming we have repeated the calculations of the  $\alpha + n$  phase shifts in a  $\{\alpha + n; d + t\}$  model space [all possible  $(L_{dt}, S_{dt})$  components are included except the  $(3, \frac{3}{2})$  one in the  $\frac{3}{2}^-$  state of  ${}^5\text{He}$ , because of the lack of the tensor force]. It turned out that the choice of the deuteron internal state is a crucial point. To be consistent with the triton we have chosen only one size parameter for the deuteron, too. The deuteron appearing in the five-nucleon system is supposed to compose a triton inside  ${}^6\text{He}$  with the additional neutron. This involves a strong restriction for the size parameter of the deuteron. To see this, we express the internal state of triton,

$$\Phi^t = \exp \left( -\frac{\beta_t}{2} \sum_{i=1}^3 (\mathbf{r}_i - \mathbf{R}_t)^2 \right) \quad (11)$$

(where  $\mathbf{R}_t$  is the triton center of mass) in terms of the  $\mathbf{r}_d = \mathbf{r}_{n_1} - \mathbf{r}_p$ ,  $\mathbf{r}_{nd} = \mathbf{r}_{n_2} - (\mathbf{r}_{n_1} + \mathbf{r}_p)/2$  and  $\mathbf{R}_t$  coordinates (where  $n_1$  and  $n_2$  denote the two neutrons)

$$\Phi^t = \exp \left[ -\frac{\beta_t}{2} \left( 3\mathbf{R}_t^2 + \frac{2}{3}\mathbf{r}_{nd}^2 + \frac{1}{2}\mathbf{r}_d^2 \right) \right]. \quad (12)$$

After this, it is obvious that the deuteron size parameter must be chosen as  $\beta_t/2$ .

TABLE IV. Point nucleon rms radii [matter ( $m$ ), neutron ( $n$ ), and proton ( $p$ )] and the thickness of the neutron halo in  ${}^6\text{He}$  (in fm).

Model	$r_m$	$r_n$	$r_p$	$r_n - r_p$
Suzuki [5]	2.40	2.64	1.82	0.82
$\{\alpha + n + n\}$	2.440	2.707	1.7790	0.917
$\{\alpha + n + n; t + t\}$	2.397	2.648	1.793	0.855
Experiment [8]	$2.48 \pm 0.03$	$2.61 \pm 0.03$	$2.21 \pm 0.03$	0.4
Experiment [9]	$2.33 \pm 0.04$	$2.59 \pm 0.04$	$1.72 \pm 0.04$	$0.87 \pm 0.06$

We have fitted two parameters of our interaction ( $u=0.92$ ,  $V_4=-691.1$  MeV) so as to get results for the  $\alpha + N$  scattering with almost the same quality as in the one-channel case (Fig. 1). (In the  $\frac{1}{2}^+$  and  $\frac{3}{2}^-$  partial waves the difference from the pure  $\alpha+n$  results are within the line thickness.) The change of the mixing parameter  $u$  slightly changes the  ${}^3P_1$  and  ${}^1P_1$   $N-N$  phase shifts as well, but these changes are all well within 0.4 deg. Using this readjusted force in the  $\{\alpha + n + n; t + t\}$  model space, we get 0.961 MeV for  ${}^6\text{He}$  which is very close to the experimental value, 0.975 MeV. To check the inherent uncertainty connected with the poorer fit of the  $\frac{1}{2}^-$   $\alpha + n$  phase shift we have selected another ( $u, V_4$ ) combination (0.94,  $-641.1$  MeV) which produces the dotted line in Fig. 1. This force gives 1.012 MeV for  ${}^6\text{He}$ ; that is, the uncertainty is as small as 0.05 MeV. The amount of  $t + t$  clustering is found to be 0.547, which confirms its major role in  ${}^6\text{He}$ . The model spaces of  ${}^6\text{Li}$  and  ${}^6\text{Be}$  have also been extended by the inclusion of a  $t+{}^3\text{He}$  and a  ${}^3\text{He}+{}^3\text{He}$  component, respectively. As we can see in Table I, the two-proton separation energy of  ${}^6\text{Be}$  also comes very close to the experiment, however, in  ${}^6\text{Li}$  approximately a 0.1-MeV is still missing. One may think that our wave function is spatially not extensive enough for such a loosely bound state. To check this we substantially extended the spatial region of our trial function, almost doubling the number of basis functions, but this yields only 0.008 MeV. This confirms that our basis is well balanced and the calculations are numerically stable. The cause of the 0.1-MeV-energy discrepancy is probably that our force reproduces just the  $p + p$  singlet  $s$ -wave effective-range parameters. It was shown [16, 17] that such a force could reproduce the  $n+n$  effective-range parameters, too, but at the same time fails to reproduce the  $p + n$  ones. In [4] it was found that the change of an  $N-N$  force, which reproduces the  $n + n$  data to another one which reproduces the  $p + n$  ones results in a  $\sim 0.18$ -MeV decrease in the two-neutron separation energy of  ${}^6\text{He}$ . This is in agreement with our finding.

We have recalculated the various radii using the readjusted force and got the results as shown in Table IV. We can see that the 0.2-MeV increase in the  ${}^6\text{He}$  two-neutron separation energy only slightly modifies the radii, that is, the neutron halo is rigid against the significant modification of the model. Finally we have carried out a calculation including the tensor interaction. The result shows that a tensor force which tends to reproduce the anomalous

phase shift order in the  ${}^3P_J$  states of the two-nucleon system, lowers the two-neutron separation energy of  ${}^6\text{He}$ . In our case this decrease is less than 0.08 MeV. We should note, however, that our  $2E_t - E_\alpha$  threshold splitting is roughly 5 MeV larger than the experimental value. This means that if this energy were right, the weight of the  $t + t$  clusterization would be higher, which would increase the two-neutron separation energy of  ${}^6\text{He}$  again. This increasing would hopefully compensate the effect of the tensor force.

## V. CONCLUSION

In summary, we have done careful microscopic multi-configuration multicluster calculations for  ${}^6\text{He}$ . We have fixed all parameters of our model to independent data, and the description of all subsystems have been found reasonably good. In respect of  ${}^6\text{He}$  our model is free of any parameter. Although our results confirm the validity of the macroscopic three-body models, we have found that the inclusion of some excited states of the  $\alpha$  particle is significant and the  $t + t$  rearrangement channel has large weight even in a model which is almost complete in the  $\alpha + n + n$  model space. The  $\alpha$  breathing modes and the  $t + t$  clusterization are found to be responsible for the missing binding energy of the macroscopic models. These effects are expected to play an important role in other halo nuclei, e.g., in  ${}^{11}\text{Li}$ . Finally we have found a very thick neutron halo in  ${}^6\text{He}$  which is in full agreement with the latest experiments [9]. We have found that this thickness is hardly sensitive to the model assumptions. Of course, the novel features of our model can really manifest their relevance in the calculation of various physical quantities (electric dipole strength,  $\beta$ -decay branching ratio, momentum distribution). These calculations as well as the application of our model to some of the above-mentioned nuclei are in progress.

## ACKNOWLEDGMENTS

This research was supported by OTKA (National Science Research Foundation, Hungary) under Contract Nos. 3010 and F4348. The author is indebted to Professor R. G. Lovas, Professor Y. Suzuki, and Dr. K. Varga for stimulating discussions and to Professor B. Gyarmati for reading the manuscript.

- [1] B. V. Danilin, M. V. Zhukov, A. A. Kostrel'nikov, and L. V. Chulkov [Sov. J. Nucl. Phys. **53**, 45 (1991)] *Yad. Fiz.* **53**, 71 (1991); B. V. Danilin, M. V. Zhukov, S. N. Ershov, F. A. Gareev, R. S. Kurmanov, J. S. Vaagen, and J. M. Bang, *Phys. Rev. C* **43**, 2835 (1991).
- [2] H. Kameyama, M. Kamimura, and M. Kawai, in *Proceedings of the International Symposium on Structure and Reactions of Unstable Nuclei* (Niigata, Japan, 1991), edited by K. Ikeda and Y. Suzuki (World Scientific, Singapore, 1991), pp. 203–210.
- [3] V. I. Kukulin, V. M. Krasnopol'sky, V. T. Voronchev, and P. B. Sazonov, *Nucl. Phys.* **A453**, 365 (1986); V. I. Kukulin, V. N. Pomerantsev, Kh. D. Rasikov, V. T. Voronchev, and G. G. Ryzhikh, Australian National University Report No. ANU-ThP-1/92 (1992).
- [4] D. R. Lehman and W. C. Parke, *Phys. Rev. C* **28**, 364 (1983); W. C. Parke and D. R. Lehman, *ibid.* **29**, 2319 (1984).
- [5] Y. Suzuki, *Nucl. Phys.* **A528**, 395 (1991).
- [6] P. Descouvemont and D. Baye, *Phys. Lett.* **292B**, 235 (1992).
- [7] A. Csóto and R. G. Lovas, *Phys. Rev. C* **46**, 576 (1992).
- [8] I. Tanihata, H. Hamagaki, O. Hashimoto, Y. Shida, N. Yoshikawa, K. Sugimoto, O. Yamakawa, T. Kobayashi, and N. Takahashi, *Phys. Rev. Lett.* **55**, 2676 (1985); I. Tanihata, H. Hamagaki, O. Hashimoto, S. Nagamiya, Y. Shida, N. Yoshikawa, O. Yamakawa, K. Sugimoto, T. Kobayashi, D. E. Greiner, N. Takahashi, and Y. Nojiri, *Phys. Lett.* **160B**, 380 (1985); I. Tanihata, T. Kobayashi, O. Yamakawa, S. Shimoura, K. Ekuni, K. Sugimoto, N. Takahashi, T. Shimoda, and H. Sato, *Phys. Lett. B* **206**, 592 (1988).
- [9] I. Tanihata, D. Hirata, T. Kobayashi, S. Shimoura, K. Sugimoto, and H. Toki, *Phys. Lett. B* **289**, 261 (1992).
- [10] M. V. Zhukov, B. V. Danilin, D. V. Fedorov, J. M. Bang, I. J. Thompson, and J. S. Vaagen, Report No. NORDITA-92/90 N.
- [11] P. N. Shen, Y. C. Tang, Y. Fujiwara, and H. Kanada, *Phys. Rev. C* **31**, 2001 (1985).
- [12] R. Beck, F. Dickmann, and A. T. Kruppa, *Phys. Rev. C* **30**, 1044 (1984).
- [13] M. Kamimura, *Prog. Theor. Phys. Suppl.* **68**, 236 (1980).
- [14] H. A. Bethe and P. Morrison, *Elementary Nuclear Theory* (Wiley, New York, 1956), pp. 59–61.
- [15] A. B. Volkov, *Nucl. Phys.* **74**, 33 (1965).
- [16] H. Eikemeier and H. H. Hackenbroich, *Nucl. Phys.* **A169**, 407 (1971).
- [17] R. V. Reid, *Ann. Phys. (N.Y.)* **50**, 411 (1968).
- [18] D. R. Thompson, M. LeMere, and Y. C. Tang, *Nucl. Phys.* **A268**, 53 (1977).
- [19] I. Reichstein and Y. C. Tang, *Nucl. Phys.* **A158**, 529 (1970).
- [20] R. A. Arndt, R. H. Hackman, and L. D. Roper, *Phys. Rev. C* **15**, 1002 (1977).
- [21] P. Heiss and H. H. Hackenbroich, *Phys. Lett.* **30B**, 373 (1969).
- [22] G. Blüge and K. Langanke, *Phys. Rev. C* **41**, 1191 (1990); *Few-Body Systems* **11**, 137 (1991); A. Csóto, R. G. Lovas, and A. T. Kruppa, *Phys. Rev. Lett.* **70**, 1389 (1993).
- [23] J. E. Bond and F. W. K. Firk, *Nucl. Phys.* **A287**, 317 (1977).
- [24] F. Ajzenberg-Selove, *Nucl. Phys.* **A490**, 1 (1988).
- [25] R. Beck, F. Dickmann, and R. G. Lovas, *Ann. Phys. (N.Y.)* **173**, 1 (1987).
- [26] R. G. Lovas and M. A. Nagarajan, *J. Phys. A* **15**, 2383 (1982).
- [27] R. G. Lovas, A. T. Kruppa, R. Beck, and F. Dickmann, *Nucl. Phys.* **A474**, 451 (1987).
- [28] A. Csóto and R. G. Lovas, in *Book of Abstracts, International Nuclear Physics Conference* (Wiesbaden, Germany, 1992), edited by U. Grundinger (GSI, Darmstadt, 1992), p. 1.4.8.